Talanta Open 11 (2025) 100439

Contents lists available at ScienceDirect

Talanta Open

journal homepage: www.sciencedirect.com/journal/talanta-open

Castor oil-based molecularly imprinted nanoparticles for the detection of cardiac troponin I: Towards green molecularly imprinted nanoreceptors

Pinar Cakir Hatir [a,*], Alice Marinangeli [b], Alessandra Maria Bossi [b], Gokhan Cayli [c]

[a] Department of Biomedical Engineering, Faculty of Engineering and Natural Sciences, İstinye University, Ayazağa Mah. Azerbaycan Cad. (Vadistanbul 4A Blok) 34396 Sariyer, İstanbul, Türkiye
[b] Department of Biotechnology, University of Verona, Strada Le Grazie 15, 37134 Verona, Italy
[c] Department of Engineering Sciences, Istanbul Cerrahpasa University, Avcilar Campus, 34320, Istanbul, Türkiye

ARTICLE INFO

Keywords:
Protein recognition
Plant-oil based functional monomer
Castor oil
Acrylated methyl ricinoleate
Molecular imprinting
Cardiac troponin I
Myocardial infarction

ABSTRACT

Molecularly imprinted polymers (MIPs) are synthetic materials that selectively recognize target molecules, offering cost-effective and stable alternatives to antibodies. While MIP nanoparticles are ideal for biomedical applications for their high surface area and their biomolecule-compatible size, traditional monomers used in their synthesis can pose issues in biocompatibility. This study presents a sustainable approach to MIP nanoparticle production using acrylated methyl ricinoleate (AMR), a functional monomer derived from castor oil. These "GreenNanoMIPs" were designed to recognize cardiac troponin I (cTnI), a key biomarker for cardiovascular events. The nanoparticles, with an average size of 81 nm, exhibited exceptional homogeneity in suspension, with a low PDI value of 0.064, and outstanding stability, as no changes in particle size distribution or PDI were observed even after one year. GreenNanoMIPs did recognize the entire cTnI protein thorough the epitope approach. Furthermore, GreenNanoMIPs were successfully used for the detection of the cTnI biomarker directly in serum. The study highlights the potential of eco-friendly, biocompatible MIPs for applications in diagnostics, drug delivery, and environmental sensing.

Introduction

Molecularly imprinted polymers (MIPs) are custom-designed synthetic materials created by means of a template-based synthesis [1,2]. Characteristic of the imprinting process is that the targeted molecule takes the role of a template and establishes specific molecular interactions with functional monomers, when co-solvated. Then, the polymerization is started by the addition of a crosslinker and of the initiator. At the completion, the template is removed, leaving on the formed material molecular cavities complementary, specific and selective for the targeted molecule. MIPs demonstrate superior availability, stability, and resistance to acidic and basic media, as well as to organic solvents, when compared to biomolecules. Additionally, they offer a cost-effective alternative for various applications.

MIPs when prepared of nanometric sizes, i.e. nanoMIPs, gain the typical features of nanomaterials, which have high area-to-volume ratio and bear a low number of binding sites per nanoMIP particle, due to the restricted dimensions, making them resemble to antibodies. The nanoMIPs have dimensions closer to that of biomolecules, enhancing their effectiveness in the biological interactions. As a result, when it comes to biomedical applications nanoMIPs have demonstrated significant potential as biosensors, diagnostics tools, therapeutics and theranostics [3–5], letting suppose widespread applications of nanoMIPs in the biomedical fields in the forthcoming future [6].

In the development of MIPs materials, prioritizing sustainable and less toxic chemical processes and materials supports a transition toward safer, eco-friendly technologies that align with green chemistry principles, ensuring minimal environmental impact while enhancing material safety for biomedical and environmental applications [7]. Along this line, tools to evaluate the overall sustainability of the MIP have been proposed [8]. Traditional monomers used for MIP syntheses can raise concerns due to their potential toxicity and persistence in the environment and eventually in individuals. By shifting to renewable, non-toxic monomers, MIP production can align with green chemistry principles, promoting safer materials for applications such as drug delivery, diagnostics, and environmental sensing. This approach supports both environmental sustainability and human health, paving the way for eco-friendly innovations in MIP technology. In particular, circular

* Corresponding author.
E-mail address: pinar.hatir@istinye.edu.tr (P. Cakir Hatir).

https://doi.org/10.1016/j.talo.2025.100439
Received 19 December 2024; Received in revised form 14 March 2025; Accepted 19 March 2025
Available online 22 March 2025

economy approaches based on the use of raw materials as sources of building blocks for polymer production has increased [9] and can open to whole new libraries of monomers for the synthesis of MIPs, where, depending on the intended applications, functional monomers and crosslinkers can be derived from various renewable materials. Even though, using green approaches in MIP synthesis and applications offer promising new opportunities, studies performed on the synthesis of MIPs using renewable resources and environmentally friendly synthesis methods are still limited.

Natural polymers like chitosan and cellulose have been explored for MIP synthesis as renewable resources in the last years [10,11]. Beyond natural polymers, plant oils also represent a promising option as renewable resources. Le Goff and coworkers developed novel bio-based MIPs using epoxidized soybean oil acrylate, as a plant oil-based cross-linker, for the controlled delivery of antifungal compounds [12]. Fatty acids, a key component of plant oils, are particularly promising for synthesizing various monomers and tailored polymers due to their potential functionality. Furthermore, compared to petroleum-based raw materials, renewable raw materials may offer natural polymer networks, resulting in improved biocompatibility and fewer immunological reactions. Consequently, plant-oil based renewable resources are often considered more suitable for biomedical applications [13,14]. To date, no fatty acid has been employed in the synthesis of molecularly imprinted polymers. In this study, we present the use of a fatty acid-derived functional monomer for the first time. Acrylated methyl ricinoleate (AMR), a functional monomer derived from castor oil, was employed in the synthesis of green molecularly imprinted polymer nanoparticles (GreenNanoMIPs).

Proteins serve as crucial analytical markers for diagnosing diseases, offering insights into the onset, progression, severity and therapeutic responses of various medical conditions. In the present work, we targeted the cardiac troponin I protein (cTnI), whose presence in blood is

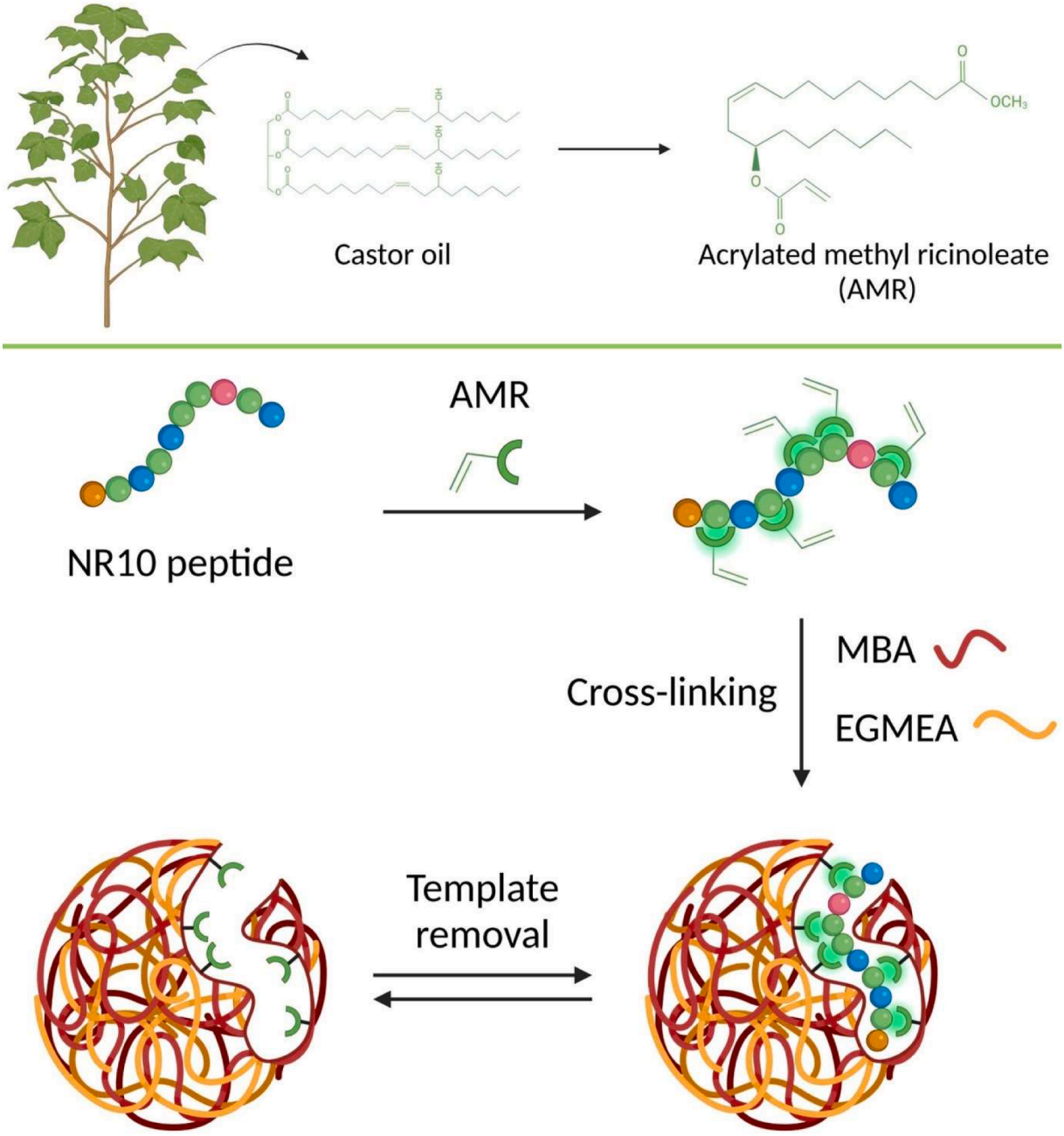

Fig. 1. Scheme of the synthesis of GreenNanoMIP selective for the cardiac troponin I protein recognition, starting from sustainable monomers derived from plant oil.

associated with cardiovascular events and in particular with myocardical infarction (MI) [15]. The cTnI enables to detect the onset of a MI event, because of its cardiac specificity, thus elevated circulating levels of cTnI strongly correlate to heart muscle damage. Additionally, cTnI allows for an early detection of MI, as its levels start to rise within a few hours after the onset of myocardial injury (typically 3–6 h). Moreover, cTnI can remain elevated for up to 10–14 days after the MI, allowing for the detection of recent myocardial damages even if in the case of delays from the patient in seeking medical care, thus being considered a marker both sensitive and of long duration. Finally, cTnI is an accurate marker, characterized by high sensitivity and specificity, thus suitable to reduce false positives and give a clearer indication of MI compared to other markers, such as creatine kinase and myoglobin. In order to prepare MIPs for the selective binding of cTnI, protein imprinting strategies were herein exploited [16]. In particular, the chosen approach was to select as template a unique peptide of cTnI, relying on the so-called epitope imprinting [17,18]. Epitopes are stretches of sequential aminoacids, mostly located in turns, loops, or at the termini of the protein structure. Ideal epitope-templates are oligopeptides, with a typical length of 8–20 aminoacids. The epitope, being a peptide with no precoined fold, withstands a broad range of polymerization conditions without alteration. Additionally, epitopes are cost-effectively produced by artificial synthesis, making the protein-recognizing MIPs significantly cheaper than antibodies [19]. The present study aims to synthesize nanoMIPs using a plant oil-derived functional monomer for the targeted recognition of cTnI. Acrylated methyl ricinoleate, obtained from castor oil, was employed as the functional monomer and used for the synthesis of cTnI nanoMIP, as schematized in Fig. 1. The resulting MIP nanoparticles were called GreenNanoMIPs. It is anticipated that GreenNanoMIPs demonstrated successful recognition of the cTnI protein through the epitope approach even in serum.

Experimental section

Materials and methods

Acrylated methyl ricinoleate (AMR) was synthesized from castor oil as described in our previous work [13]. All solvents, Ethylene glycol methyl ether acrylate (EGMEA), Lithium phenyl-2,4,6-trimethylbenzoylphosphinate (LAP), N, N′-Methylenebis(acrylamide) (MBA) and Human serum albumin (HSA) were purchased from Sigma-Aldrich (Darmstadt, Germany). Cardiac troponin I (cTnI) was purchased from GenScript. The peptides NR10 of sequence NIDALSGMGR, the NR10 labelled with fluorescein (FITC-NIDALSGMGR), NR11 of sequence NIDALSGMEGR and FN11 of sequence FGSNVTDCSGN were custom synthesized from TAG-Copenhagen. DMSO, ultra-pure water and PBS 10 mM pH 7.4 (filtered) were used. The chemical structures of polymer nanoparticles were evaluated using Jasco 4600 Fourier Transform Infrared Spectroscopy (FTIR) with a wavenumber range of 400–4000 cm^{-1}. Morphology of nanoparticles was investigated using JCM-5000 NeoScope QUATTRO S scanning electron microscope (SEM). Particle size distribution was investigated by Dynamic Light Scattering (Malvern Zetasizer Nano ZS). Time-resolved fluorescence intensities were collected using a single photon counting spectrometer Nanolog/Fluorolog-3-2iHR320 (Horiba-Jobin Yvon, Kyoto, Japan).

Synthesis of GreenNanoMIPs

AMR, EGMEA and the template-peptide solution (as shown in Table SI1) were mixed and left for 15 min to form an intermolecular complex via noncovalent interactions. Then, the required amount of solvent composition (90:10, DMSO:H_2O) was transferred into each reaction medium inside a glass vial. The monomer concentration was kept at 0.5 % (wt/wt). MBA and the initiator (10 % wt/wt, of the final weight of the monomers) were subsequently added. The vials were placed under an LED UV lamp (365 nm). After 2 min of UV irradiation, the reaction was terminated. Each solution then received 2 mL of Tris free base (50 mM) and was left in the dark for 30 min. The polymerization solutions were then transferred into dialysis membranes (12000 Da MWCO) and dialyzed against 5 L of water, repeated three times. Finally, the solutions were transferred into falcon tubes and freeze-dried. Non-imprinted polymer nanoparticles were synthesized using the same method in the absence of the peptide.

Fluorescence lifetime measurements

The fluorescence lifetime of a population, measured in the time-domain, follows the equation:

$$I(t) = I_0 e^{-t/\tau}$$

where $I(t)$ is the intensity at time t; I_0 is the intensity at t = 0; t is the time after the absorption; and τ is the fluorescence lifetime. Time-resolved fluorescence intensities were collected using a single photon counting spectrometer Nanolog/Fluorolog-3-2iHR320 (Horiba-Jobin Yvon, Kyoto, Japan) equipped with a NanoLED source with a wavelength of 453 nm. The emission was monitored at the angle of 90° with respect to the excitation. Data were collected in 1023 channels to 10,000 counts in the peak, while the calibration time was 109.73 ps per channel. The voltage at the photomultiplier (PTM) was set to 950 V. Measurements were performed in a 1 mL quartz cuvette, using a fixed concentration of NR10-FITC (10 nM) diluted in PBS (10 mM pH 7.4), adding increasing concentrations of NPs (0.5 ng/mL–5000 ng/mL). A 10 nM of NR10-FITC was excited at λ_{exc}= 453 nm to obtain the instrumental response (prompt) for the deconvolution. The sample decays were recorded at λ_{em}= 522 nm.

Data were elaborated with the Decay Analysis Software V. 6.8 (Horiba Scientific, Yvon, Kyoto, Japan), choosing a biexponential fitting equation model:

$$I(t) = A + B_1 e^{-t/\tau 1} + B_2 e^{-t/\tau 2}$$

The lifetime values (τ_2), plotted as a function of NPs concentration, described the binding isotherm for the interaction. Data were fitted with the Hill equation model (OriginPro 9.0):

$$\tau_2 = \tau_{2\_max} \frac{x^n}{(K + x^n)}$$

where τ_2 is the lifetime at concentration x of the ligand; τ_2_max is the τ value at binding saturation; n is the Hill parameter, which correlates with the number of binding sites, and K is the apparent dissociation constant.

Selectivity test

Different competitors were chosen to test the selectivity of NPs: NR10 (NIDALSGMGR), NR11 (NIDALSGMEGR) and FN11 (FGSNVTDCSGN). A solution of NPs at the final concentration of 25 ng/mL was incubated with a fixed concentration of NR10-FITC (10 nM). Competitors were added to this solution at different concentrations (10 nM, 100 nM, 1μM and 10 μM) to study the displacement of the analyte NR10-FITC. Additionally, the ability of NPs to bind the target protein (cTnI) and with a non-target protein (HSA) was tested using the concentrations of 100 nM and 1 μM. Fluorescence lifetime was measured as explained above. Measurements were performed in triplicate.

Lifetime measurements in human serum

Human serum from a pool of healthy donors was diluted 1:50. Measurements were performed by recording the τ_2 of NR10-FITC at the final concentration of 10 nM. The NPs were dispersed in serum at the concentration of 25 ng/mL, added of NR10-FITC (10 nM), and lifetime

was measured. Finally, serum with NPs (25 ng/mL) and NR10-FITC (10 nM) was spiked with 1 μM of cTnI and τ_2 was recorded.

Results and discussion

Synthesis and characterization of MIP nanoparticles

Castor oil-based monomers, acrylated methyl ricinoleate (AMR), synthesized as reported in our previous work [13] were employed to the synthesis of GreenNanoMIPs. The peptide epitope used as a template has a combination of hydrophilic and hydrophobic groups, therefore in designing the synthetic mixture for the MIP synthesis, a combination of a hydrophobic sustainable monomer AMR and of a hydrophilic monomer EGMEA was used. Initially, the synthetic space was explored by testing a range of conditions (Table S1), which included to vary the molar ratios of the sustainable monomer, AMR, and of the hydrophilic monomer EGMEA (either 9:1 or 1:1 molar ratio) and to inspect whether the presence or the absence of the crosslinker MBA had an effect, finally nanoparticles were synthesized both in the presence or absence of the template. GreenNanoMIPs were respectively called I, when the AMR monomer used was at a 45 % molar ratio, and as II when AMR was used at a 25 % molar ratio. All the nanoparticles were synthesized in an aqueous solution (10 % DMSO) using a high-dilution method under UV irradiation [20,21]. Specifically, the prepolymerization solution contained a total monomer concentration of 0.5 % (wt/wt) to ensure a highly diluted medium, that is known as one of the most used and straightforward methods for producing monodisperse nanoparticles. At the end of the reaction, GreenNanoMIPs I and II and its controls were observed to yield to monodisperse and stable nanomaterials, as indicated by the sizes below 100 nm and the PDI values below 0.2, and in some cases below 0.1, measured at DLS (Fig. 2). Considering that GreenNanoMIP II and Control NP II have an equal molar ratio of hydrophobic and hydrophilic moieties, whereas GreenNanoMIP I and Control NP I contain a higher proportion of hydrophobic moieties, the difference in the PDIs observed between the nanoparticles I and II may be related to the respective monomer compositions. Higher proportion of hydrophobic groups can promote more uniform growth. However, nanoparticles with an equal hydrophilic-hydrophobic balance may grow at different rates in distinct solubility regions, leading to increased polydispersity (Table SI1). Finally, in the absence of the crosslinker, large, polydisperse polymer particles exhibiting sedimentation were produced. In the presence of the crosslinker, monodisperse nanoparticles with low PDI were obtained.

The polymerization yields of GreenNanoMIPs and Control NPs were determined by the ratio of the weight of the NPs after lyophilization respect to the total weight of the monomers used in the reaction, multiplied by 100. Fig. 2B reports the yield % of GreeenNanoMIPs and of the control NPs. For both samples, GreenNanoMIP I and GreenNanoMIP II, the imprinted polymer nanoparticles exhibited higher polymerization yields of 92.8 % and 86.4 %, respectively, compared to their corresponding non-imprinted controls, Control NP I and Control NP II. The presence of the template molecule likely facilitates the formation of a stable complex, maintaining the proximity of the functional monomers and consequently resulting in an increased polymerization yield. Additionally, it was also observed that the polymerization yield appeared to increase with increasing AMR molar ratio.

FTIR spectra of the polymer nanoparticles are shown in Fig. 2A. All the spectra fully overlap, indicating the polymer nanoparticles have the same composition. In the spectra of the polymer nanoparticles, a strong peak at 1725 cm^{-1} is observed, corresponding to saturated ester moieties arising from the ricinoleate ester carbonyl and the polymerization of acrylate groups in AMR and EGMEA. The presence of a single ester peak, rather than two distinct ester carbonyl peaks, confirms the absence of unreacted acrylate ester carbonyl groups in the polymer nanoparticles [13]. Amide I and amide II bands are visible at 1649 and 1527 cm^{-1}. The intensity of the broad band observed at around 3300 cm^{-1}, caused by NH stretching of secondary amide. Scanning electron microscopy (SEM) was utilized to perform the morphological analysis of GreenNanoMIPs. Fig. 2C and D present SEM images of GreenNanoMIPs at low and high magnifications, respectively. The SEM analysis reveals well-defined, monodisperse spherical nanoparticles.

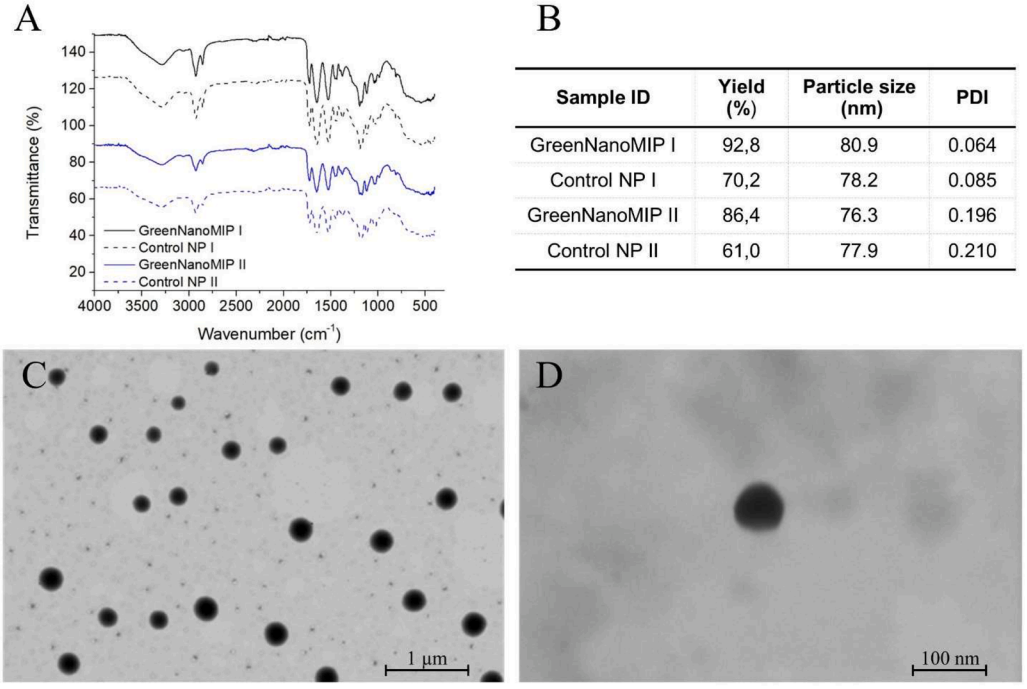

Sample ID	Yield (%)	Particle size (nm)	PDI
GreenNanoMIP I	92,8	80.9	0.064
Control NP I	70,2	78.2	0.085
GreenNanoMIP II	86,4	76.3	0.196
Control NP II	61,0	77.9	0.210

Fig. 2. A: FTIR spectra of GreenNanoMIPs and Control NPs; B: the yield (%), the particle size and the PDI of GreenNanoMIPs and Control NPs; C and D: SEM images of GreenNanoMIP I.

Particle size distribution

The size distribution of the synthesized GreenNanoMIPs and control NPs was determined by dynamic light scattering (DLS) technique. Polymer nanoparticles were tested after dialysis. The average particle sizes and polydispersity index values (PDI) are exhibited in Fig. 2B. GreenNanoMIP I, Control NP I, GreenNanoMIP II and Control NP II have average particle sizes of 80.9 nm, 78.2 nm, 76.3 nm and 77.9 nm, respectively. GreenNanoMIP I exhibited a remarkable homogeneity, having a PDI value as low as 0.064, which is significantly unusual for polymeric NPs. It should be noted that, even though all the NP solutions have monodispersed character with only one population, GreenNanoMIP II and Control NP II have higher PDI with larger particle population. In general, it was observed that PDI of the NPs decreased with increasing AMR molar ratio.

Stability of GreenNanoMIP in aqueous dispersion

GreenNanoMIP I and II and their controls were solvated in distilled water at 1 mg/mL concentrations. The solutions were kept at 4 °C and measured over time, up to after 1 year. Fig. 3 demonstrates the outstanding stability of the formed NPs, as there was no change in particle size distribution or PDI after one year. Notably, the solutions remained free from sedimentation or agglomeration. Additionally, particle size distribution analyses were performed under various conditions to assess the stability of nanoparticles for potential applications. The size distributions were measured at pH 4.0, pH 8.5, and 40 °C (Fig. SI2). With increasing temperature, the nanoparticles exhibited a slight reduction in size, confirming their thermoresponsive nature. At pH 8.5, they became larger while maintaining a monodisperse character, whereas at low pH, agglomeration was observed.

Binding studies of GreenNanoMIPs by means of Fluorescence Lifetime Measurements

The ability of GreenNanoMIPs I and II to bind the target analyte was investigated by means of fluorescence lifetime decay [22]. Chosen analyte was a unique peptide of cTnI labelled with the organic fluorophore fluorescein and indicated as NR10-FITC. NR10-FITC was used at the concentration of 10 nM and was incubated with increasing concentrations, from 0.5 ng/mL to 5000 ng/mL of NPs (GreenNanoMIP I, Control NP I, GreenNanoMIP II and Control NP II). The intensity decay curve of NR10-FITC was recorded at λ_{em} = 522 nm. Data were fitted with a biexponential fitting (τ_1 and τ_2) with fixed τ_1, in similarity to experimental conditions previously optimized [22]. Data were fitted with a biexponential fitting (τ_1 and τ_2) with fixed τ_1, in similarity to experimental conditions previously optimized [22]. Indeed, this was an approximate, though acceptable, model to represent and discriminate between the decay's contributions given by the fluorescent peptides randomly placed in solution and the decay's related to fluorescent peptides effectively bound to the imprinted binding sites of the GreenNanoMIPs. In detail, a fixed τ_1 was used as a global descriptor of all the non-specific decays occurring outside the molecularly imprinted cavities, whereas the binding-related interactions were observed as τ_2. Fig. 4 shows the binding curves related to NR10-FITC incubated with increasing concentrations of NPs GreenNanoMIP I with the relative non-imprinted Control NP I (Fig. 4A) and NPs GreenNanoMIP II with the relative non-imprinted Control NP II (Fig. 4B). The fluorescence lifetime of NR10-FITC decreases upon the addition of imprinted NPs (GreenNanoMIP I and GreenNanoMIP II) whereas no variation was observed for non-imprinted NPs (Control NP I and Control NP II). This suggested that the imprinting process effectively stamped binding sites on the nanoparticles. GreenNanoMIP II showed high uncertainty in the lifetime decays, possibly given by the tendency of these NPs to form aggregates, as supported by the larger PDIs values and the standard errors. Table 1 reports the data of the GreenNanoMIP I binding curve fitted with the Hill equation model. The GreenNanoMIP I measurement's space was of ~200 ps, with a half saturation which correlates with the dissociation constant at 3.31 ng/mL. The statistical number of binding sites per particle, n, had a value of 0.45 indicating that not all the formed binding sites were accessible. Out of this evidence, GreenNanoMIP I resulted promising for nanosensing applications. Fig. 4C and D report, respectively, the nonlinear fitting and the fitting with a linear equation model of just the linear portion of the binding isotherm of GreenNanoMIP I, with the parameters reported in Table 1.

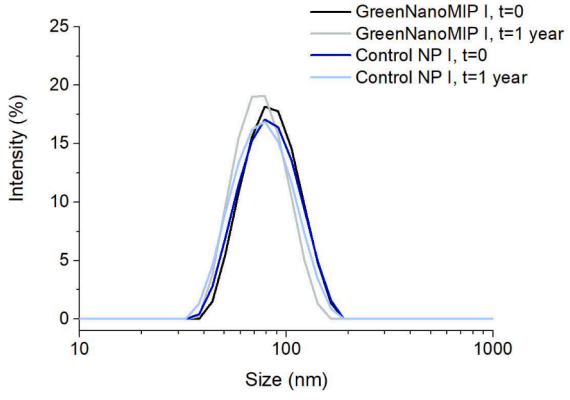

Fig. 3. Particle size distributions at the initial measurement and subsequently after one year.

Selectivity test

In order to test the binding selectivity of GreenNanoMIP I, a fluorescence lifetime experiment was carried out, so to confirm that the binding to the imprinted NPs, GreenNanoMIP I, was specific and selective for the targeted analyte (i.e. the cTnI peptide NR10). The peptides chosen as competitors were compared for their physicochemical characteristics, as reported in Table SI2. The target peptide NR10 is characterized by an isoelectric point (pI 7.00) alike its labelled form NR10-FITC, that was used as a probe for the lifetime measurements. In contrast, NR11 and FN11 peptides which are characterized by lower pIs, 4.07 and 3.12 respectively, were chosen to devise the effect of charge on NPs binding.

For the competition experiment, a solution of GreenNanoMIP I (25 ng/mL) was incubated with a fixed concentration of NR10-FITC (10 nM), in a condition that saturates the available binding sites. Then, each competitor, i.e. the non-fluorescent target NR10 and the non-related peptides NR11 and FN11, was added at the molar ratios of 1:1, 10:1, 100:1 and 1000:1 with respect to NR10-FITC. As shown in Fig. 5A, the incubation of the mix NPs GreenNanoMIP I and NR10-FITC with NR10 produced a drop of the fluorescence lifetime, indicating a displacement of the NR10-FITC as expected. In contrast, the incubation with non-template peptides did not produce significant changes in the τ_2, demonstrating the selectivity of the NPs GreenNanoMIP I *versus* the targeted peptide.

Overall, these tests allowed to get insights into the key mechanisms of the molecular recognition between NR10 and the GreenNanoMIPs I. In fact, the peptides NR11 and FN11 had molecular weight's values close to that of the template NR10, but different sequences, showing the binding is mainly driven by the sequence recognition than by the peptide's length. The sequence effect was investigated more in details using the peptide NR11, which share the same sequence of NR10, with the addition of a single aminocid (a glutamic acid within the sequence). As a result, the presence of a single aminoacid can be disruptive for the binding, especially if this produces a change in the pI of the peptide. Concerning the pI, NR10 was close to neutrality, whereas the competitor peptides were mild acidic, this showed that the effect of charge on the binding is crucial. The effect of hydrophobicity with its correlating GRAVY parameter, supported a favorable binding to GreenNanoMIP I for NR10, slightly more hydrophobic than NR11 and FN11.

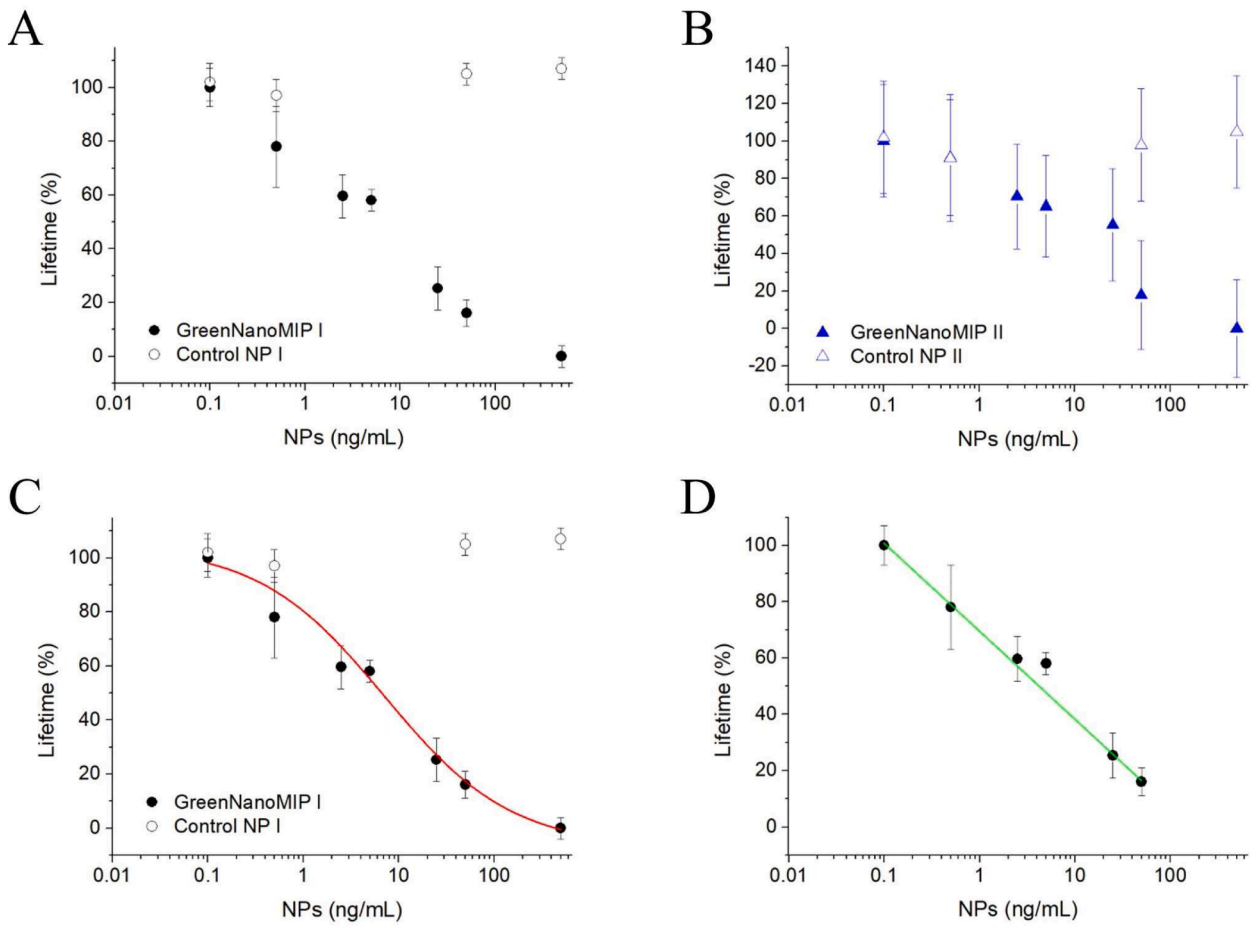

Fig. 4. A: Imprinted and control NPs incubated with increased concentrations of NR10-FITC (GreenNanoMIP I and Control NP I); B: Imprinted and control NPs incubated with increased concentrations of NR10-FITC (GreenNanoMIP II and Control NP II). C Imprinted NPs binding curve fitted with Hill equation model (red line) and (D) linear (green line) equation model.

Table 1
Binding values from the Hill and linear equation model.

Parameters	GreenNanoMIP I
τ_{2_0} (ns)	3.7633 ± 0.0396
τ_{2_max} (ns)	3.5259 ± 0.0252
EC_{50} (ng/mL)	3.3162 ± 0.0444
n	0.4527 ± 0.0164
R^2_{adj}	0.98531
Parameters	GreenNanoMIP I
Intercept	3.6656 ± 0.0009
Slope	–0.0528 ± 0.0005
R^2_{adj}	0.99959

In order to prove the effectiveness of the epitope-imprinting strategy hence the formation of imprinted binding sites in GreenNanoMIP I suitable to recognize the whole cTnI protein, the binding of cTnI to GreenNanoMIP I was tested in a competitive experiment in fluorescence lifetime, using NR10-FITC as a fluorescent probe and results were compared to the ability of GreenNanoMIP I in rebinding a MI non-related protein, that was human serum albumin (HSA) and was chosen for its abundance in serum, that might be the specimen next used for testing patients for suspected MI. Fig. 5B shows that the whole protein biomarker, cTnI, produced a clear displacement of the NR10-FITC probe. In contrast, HSA did not show a dose-related displacement, but possibly a minor and non-specific adsorption effect. Overall, these results clearly indicate the epitope approach proved effective, as the NR10 imprinted GreenNanoMIPs demonstrated to bind selectively the whole cardiac Troponin I protein (Fig. 5B). As a further control of the specific and selective binding, control non-imprinted NPs (Control NP I) were tested in a competition experiment in fluorescent lifetime and using NR10-FITC as a probe. The results, reported in in Fig. 6 showed that NPs Control NP I do not bind the fluorescent probe, as indicated by the non-significative change in the τ_2 upon NPs addition. Moreover, proteins, both the target cTnI and serum albumin, produced the same and concentration independent effect on the measurement. These results strongly support the non-specific character of the Control NPs, respect to the imprinted GreenNanoMIPs.

Measurements in human serum

Finally, the ability of GreenNanoMIPs to rebind the targeted biomarker in serum was also tested. A sample of pooled sera from healthy volunteers (Sigma-Merck) was diluted and spiked with a known concentration of cTnI (1 μM). Sera, control and the cTnI spiked one, were then incubated with a known concentration of GreenNanoMIP I (25 ng/mL) and a known quantity of NR10-FITC probe. Lifetime measurements results are reported in Fig. 7. It can be appreciated that the GreenNanoMIP I and NR10-FITC fluorescent probe provide a determination method that can be used in serum, opening to the development of GreenNanoMIP I nanosensors assays, Additionally, these preliminary results show that the GreenNanoMIP I competitive strategy indeed provided the detection of the biomarker cTnI directly in serum (Fig. 7).

GreenNanoMIP I enabled to determine cTnI directly in serum without pre-treatments, despite optimization is needed to achieve lower detection limits. In the literature, there are examples of MIP-based

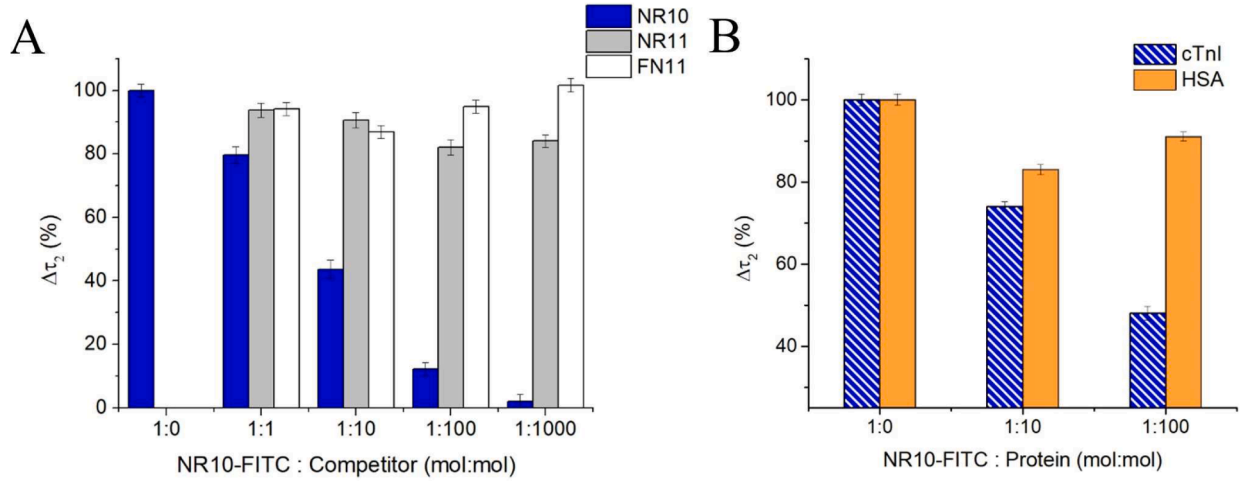

Fig. 5. A: selectivity of GreenNanoMIP I NPs using different peptide; B: Selectivity test of GreenNanoMIP I using different protein.

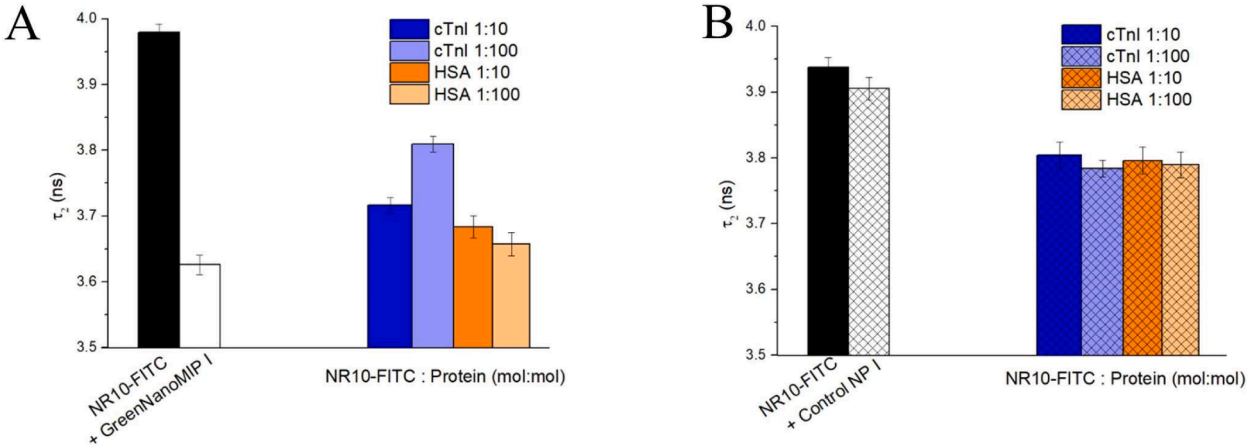

Fig. 6. Competitive lifetime experiments to evaluate the selectivity of GreenNanoMIP I NPs and of Control NP I. A: lifetime decay of NR-10-FITC only (solid black bar); upon the addition of GreenNanoMIP I NPs (white bar); upon the addition of competitors to the NR-10-FITC + GreenNanoMIP I NPs, namely cTnI 10x blue or 100x light blue; HSA 10x orange or 100x light orange; B: lifetime decay of NR-10-FITC only (solid black bar); upon the addition of Control I NPs (white striped bar); and upon the addition of competitors to the NR-10-FITC + Control I NPs, namely cTnI 10x striped blue or 100x striped light blue; HSA 10x striped orange or 100x striped light orange.

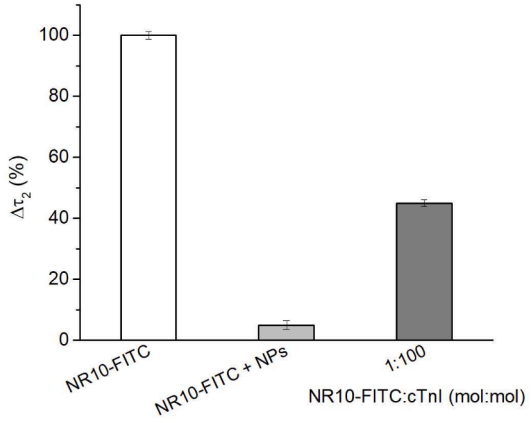

Fig. 7. Lifetime competitive measurements of spiked cTnI in human serum. White bar: NR10-FITC in cTnI depleted serum; light grey bar: NR10-FITC in cTnI depleted serum upon the addition GreenNanoMIP I; dark grey bar: GreenNanoMIP I particles added to NR10-FITC in serum spiked with cTnI.

sensing of cTnI, as reported in Table 2, mostly with electrochemical transduction. However, to attain the LODs required in clinical assessments often samples are pretreated, either centrifugated or enriched by preconcentration steps on columns.

At last, a comparison was made between GreenNanoMIP I and others, more traditional, MIP materials, equally prepared for the recognition of cTnI. It was observed that castor-oil based MIP nanoparticles displayed an affinity for cTnI of about 3×10^{11} M^{-1}, which was alike, or superior to that reported for traditional MIPs. In particular, the group of Altintas prepared p-NIPAM-co-APM in the form of nanoMIPs, with a reported affinity for cTnI of 3×10^{10} M^{-1} [23] and later electropolymerized a MIP in the form of a thin layer, made staring from 2-Aminophenol, that exhibited an affinity of 5×10^{11} M^{-1} [25]. These results support the competitivity of the GreenNano MIPs, made starting from more sustainable building blocks, in terms of affinity of the interaction.

Conclusions

In this study, we introduce a fatty acid-derived functional monomer for the first time in the synthesis of MIP nanomaterials. Acrylated methyl ricinoleate (AMR), derived from castor oil, was utilized in the synthesis

Table 2
Literature examples of MIP-based sensing of cTnI.

MIP NPs type	MIP composition	Detection	Range concentration	LOD	Reference
MIP immobilized on Au surface	NIPAm[a] APM[b]	SPR	0.78–50 ng/mL	0.52 ng/mL	[23]
MIP/QDs/GCE	Pyrrole	DPV	0.01–5 ng/mL	0.0005 ng/mL	[24]
MIP electropolymerized layer	2-AP[c]	SWV	0.005–10 ng/mL	0.5 pg/mL	[25]
MIP electropolymerized layer on GCE	DA[d]	ECL	$0.005–10^4$ ng/mL	0.0184 ng/mL	[26]
GCE/MIP	O-AP[e]	EIS	0.05–5 nM	0.027 nM	[27]
MIPs layer/MWCNTs/GS on GCE	MAA[f]	DPV	0.005 to 60 ng/mL	0.0008 ng/mL	[28]
Magnetic MIP	MAA[f] DMAm[g]	Raman spectroscopy	0.001–100 ng/mL	0.063 pg/mL	[29]
GreenNanoMIP	AMR, EGMEA	Fluorescence LT	0.1–50 ng/mL	1.6 ng/mL	This work

[a] N-Isopropylacrylamide
[b] N-(3-Aminopropyl) methacrylamide hydrochloride
[c] 2-Aminophenol
[d] Dopamine
[e] O-Aminophenol
[f] Methacrylic acid
[g] N,N-Dimethylacrylamide.

of environmentally friendly molecularly imprinted polymer nanoparticles (GreenNanoMIPs). By employing a renewable, plant-oil-based monomer, we successfully developed a sustainable method to produce green nanoMIPs. The use of this castor oil-based monomer not only supports an eco-friendly approach but also yields a biocompatible and non-immunogenic natural biomaterial. Recently Martine Esteban proposed a method to measure the greenness of MIPs with a score system [8], which in the case of GreenNanoMIPs resulted very low (Fig. S1).

Additionally, here the greener nanoMIPs were specifically addressed at targeting the cardiac troponin I (cTnI), a protein marker in the blood associated with cardiovascular events, particularly myocardial infarction (MI). Stable, monodisperse GreenNanoMIPs were produced, that demonstrated successful recognition of the cTnI protein through an epitope approach. The GreenNanoMIPs demonstrate ability to bind cTnI even in serum, suggesting high selectivity of the nanomaterials imprinted. These MIP nanoparticles align with green chemistry principles, advancing safer materials for applications in drug delivery, diagnostics, and environmental sensing.

Author contributions

The manuscript was written through contributions of all authors. All authors have given approval to the final version of the manuscript. These authors contributed equally.

Funding sources

This research was supported by Istinye University Scientific Research Projects (2022/GBAP3) and the Italian Ministry of Research and University with the PON PNRR D.M.351 funds.

Abbreviations

MIPs, molecularly imprinted polymers; SEM, scanning electron microscopy; FTIR, Fourier-transform infrared; AMR, acrylated methyl ricinoleate; cTnI, cardiac troponin I protein; MI, myocardical infarction, PBS, Phosphate-buffered saline.

Supplementary material

Synthetic space: molar equivalency % of the synthetic reagents and physical characteristics of the produced nanoparticles, physicochemical characteristics of the target peptide epitope and of selected competitors and green score for the GreenNanoMIP (PDF).

CRediT authorship contribution statement

Pinar Cakir Hatir: Writing – review & editing, Writing – original draft, Validation, Supervision, Methodology, Investigation, Funding acquisition, Conceptualization. **Alice Marinangeli:** Writing – original draft, Methodology, Investigation, Data curation. **Alessandra Maria Bossi:** Writing – review & editing, Writing – original draft, Validation, Supervision, Methodology, Investigation, Funding acquisition, Conceptualization. **Gokhan Cayli:** Writing – original draft, Project administration, Methodology.

Declaration of competing interest

The authors declare that they have no known competing financial interests or personal relationships that could have appeared to influence the work reported in this paper.

Acknowledgments

A.M.B. and A.M. acknowledge Ministry of University and Research for MUR D.M. 351 PON PNRR doctoral program. A.M.B. acknowledges the Centro Piattaforme Tecnologiche (CPT) of the University of Verona for the facilities DLS and Spectroscopy facilities. A.M.B. and P.C.H. acknowledge Verona University - Internationalisation Programme 2022. The authors also thank to Boğaziçi University's Center for Life Sciences and Technologies for conducting the SEM analyses and to Istinye University Scientific Research Projects (2022/GBAP3) for funding. The authors are grateful to Rojia Houshang for her support in conducting additional DLS measurements.

Supplementary materials

Supplementary material associated with this article can be found, in the online version, at doi:10.1016/j.talo.2025.100439.

Data availability

Data will be made available on request.

References

[1] R. Arshady, K. Mosbach, Synthesis of substrate-selective polymers by host-guest polymerization, Makromol. Chem. 182 (1981) 687–692, https://doi.org/10.1002/macp.1981.021820240.
[2] G. Wulff, A. Sarhan, Über die anwendung von enzymanalog gebauten polymeren zur racemattrennung, Angew. Chem 84 (1972) 364, https://doi.org/10.1002/ange.19720840838.

[3] B. Tse Sum Bui, K. Haupt, Molecularly imprinted polymer hydrogel nanoparticles: synthetic antibodies for cancer diagnosis and therapy, ChemBioChem 23 (2022) e202100598, https://doi.org/10.1002/cbic.202100598.
[4] A. Kumar, S. Kashyap, F. Mazahir, R. Sharma, A.K. Yadav, Unveiling the potential of molecular imprinting polymer-based composites in the discovery of advanced drug delivery carriers, Drug Discov. Today 29 (2024) 104164, https://doi.org/10.1016/j.drudis.2024.104164.
[5] Kang M.S, E. Cho, H.E. Choi, C. Amri, J.H. Lee, K.S. Kim, Molecularly imprinted polymers (MIPs): emerging biomaterials for cancer theragnostic applications, Biomater. Res. 27 (2023) 45, https://doi.org/10.1186/s40824-023-00388-5.
[6] S. Piletsky, F. Canfarotta, A. Poma, A.M. Bossi, S. Piletsky, Molecularly imprinted polymers for cell recognition, Trend. Biotechnol. 38 (2020) 368–387, https://doi.org/10.1016/j.tibtech.2019.10.002.
[7] R. Del Sole, G. Mele, E. Bloise, L. Mergola, Green aspects in molecularly imprinted polymers by biomass waste utilization, Polymers 13 (2021) 2430, https://doi.org/10.3390/polym13152430.
[8] M. Marć, W. Wojnowski, F. Pena-Pereira, M. Tobiszewski, A. Martín-Esteban, AGREEMIP: the analytical greenness assessment tool for molecularly imprinted polymers synthesis, ACS Sustain. Chem. Eng. 12 (2024) 12516–12524, https://doi.org/10.1021/acssuschemeng.4c03874.
[9] A. Martín-Esteban, Green molecularly imprinted polymers for sustainable sample preparation, J. Sep. Sci. 45 (2022) 233–245, https://doi.org/10.1002/jssc.202100581.
[10] J. Werner, A. Zgoła-Grześkowiak, T. Grześkowiak, R. Frankowski, Biopolymers-based sorbents as a future green direction for solid phase (micro)extraction techniques, TrAC - Trend. Anal. Chem. 173 (2024) 117659, https://doi.org/10.1016/j.trac.2024.117659.
[11] N.H. Godage, E. Gionfriddo, Use of natural sorbents as alternative and green extractive materials: a critical review, Anal. Chim. Acta 1125 (2020) 187–200, https://doi.org/10.1016/j.aca.2020.05.045.
[12] N. Le Goff, I. Fomba, E. Prost, F. Merlier, K. Haupt, L. Duma, A. Fayeulle, A. Falcimaigne-Cordin, Renewable plant oil-based molecularly imprinted polymers as biopesticide delivery systems, ACS Sustain. Chem. Eng. 8 (2020) 15927–15935, https://doi.org/10.1021/acssuschemeng.0c05145.
[13] P.C. Hatir, G. Cayli, Environmentally friendly synthesis and photopolymerization of acrylated methyl ricinoleate for biomedical applications, J. Appl. Polym. Sci. 136 (2019) 47969, https://doi.org/10.1002/app.47969.
[14] P.C. Hatir, Light-induced hydrogels derived from poly(ethylene glycol) and acrylated methyl ricinoleate as biomaterials, J. Appl. Polym. Sci. 139 (2022) e52754, https://doi.org/10.1002/app.52754.
[15] E. Antman, J.P. Bassand, W. Klein, M. Ohman, J.L. Lopez Sendon, L. Rydén, M. Simoons, M. Tendera, Myocardial infarction redefined—a consensus document of the Joint European Society of Cardiology/American College of Cardiology Committee for the redefinition of myocardial infarction: The Joint European Society of Cardiology/American College of Cardiology Committee, J. Am. Coll. Cardiol. 36 (2000) 959–969, https://doi.org/10.1016/s0735-1097(00)00804-4.
[16] A.M. Bossi, F. Bonini, A.P.F. Turner, S.A. Piletsky, Molecularly imprinted polymers for the recognition of proteins: the state of the art, Biosens. Bioelectron. 22 (2007) 1131–1137, https://doi.org/10.1016/j.bios.2006.06.023.
[17] A. Rachkov, N. Minoura, Towards molecularly imprinted polymers selective to peptides and proteins: the epitope approach, Biochim. Biophys. Acta Prot. Struct. Mol. Enzymol. 1544 (2001) 255–266, https://doi.org/10.1016/s0167-4838(00)00226-0.
[18] L. Pasquardini, A.M. Bossi, Molecularly imprinted polymers by epitope imprinting: a journey from molecular interactions to the available bioinformatics resources to scout for epitope templates, Anal. Bioanal. Chem 413 (2021) 6101–6115, https://doi.org/10.1007/s00216-021-03409-1.
[19] K. Kang, S. Li, L. Liu, Y. Chen, W. Zhou, J. Pei, Z. Liang, L. Zhang, Y. Zhang, Epitope imprinting technology: progress, applications, and perspectives toward artificial antibodies, Adv. Mater. 31 (2019) e1902048, https://doi.org/10.1002/adma.201902048.
[20] A. Biffis, N.B. Graham, G. Siedlaczek, S. Stalberg, G. Wulff, The synthesis, characterization, and molecular recognition properties of imprinted microgels, Macromol. Chem. Phys. 202 (2001) 163–171, https://doi.org/10.1002/1521-3935(20010101)202. :1%3C163::aid-macp163%3E3.0.co;2-m.
[21] P.Cakir Hatir, A. Cutivet, M. Resmini, B.T.S. Bui, K. Haupt, Protein-size molecularly imprinted polymer nanogels as synthetic antibodies, by localized polymerization with multi-initiators, Adv. Mater. 25 (2013) 1048–1051, https://doi.org/10.1002/adma.201203400.
[22] A.M. Bossi, A. Marinangeli, A. Quaranta, L. Pancheri, D. Maniglio, Time-resolved fluorescence spectroscopy of molecularly imprinted nanoprobes as an ultralow detection nanosensing tool for protein contaminants, Biosensors 13 (2023) 745, https://doi.org/10.3390/bios13070745.
[23] S. Choudhary, Z. Altintas, Development of a point-of-care SPR sensor for the diagnosis of acute myocardial infarction, Biosensors 13 (2023) 229, https://doi.org/10.3390/bios13020229.
[24] M.L. Yola, N. Atar, Development of cardiac troponin-I biosensor based on boron nitride quantum dots including molecularly imprinted polymer, Biosens. Bioelectron. 126 (2019) 418–424, https://doi.org/10.1016/j.bios.2018.11.016.
[25] G.K. Hasabnis, Z. Altintas, Cardiac troponin I-responsive nanocomposite materials for voltammetric monitoring of acute myocardial infarction, ACS Omega 9 (2024) 30737–30750, https://doi.org/10.1021/acsomega.4c03252.
[26] S. He, P. Zhang, J. Sun, Y. Ji, C. Huang, N. Jia, Integrating potential-resolved electrochemiluminescence with molecularly imprinting immunoassay for simultaneous detection of dual acute myocardial infarction markers, Biosens. Bioelectron. 201 (2022) 113962, https://doi.org/10.1016/j.bios.2022.113962.
[27] J. Zuo, X. Zhao, X. Ju, S. Qiu, W. Hu, T. Fan, J. Zhang, A new molecularly imprinted polymer (MIP)-based electrochemical sensor for monitoring cardiac troponin I (cTnI) in serum, Electroanalysis 28 (2016) 2044–2049, https://doi.org/10.1002/elan.201600059.
[28] Y. Ma, X.L. Shen, H.S. Wang, J. Tao, J.Z. Huang, Q. Zeng, L.S. Wang, MIPs-graphene nanoplatelets-MWCNTs modified glassy carbon electrode for the determination of cardiac troponin I, Anal. Biochem. 520 (2017) 9–15, https://doi.org/10.1016/j.ab.2016.12.018.
[29] S. Wang, J. Qin, Y. Liang, Y. Ye, Y. Guo, S. Li, Y. Liang, A magnetic SERS-imprinted sensor for the determination of cardiac troponin I based on proteolytic peptide technology, Anal. Chim. Acta 1332 (2024) 343316, https://doi.org/10.1016/j.aca.2024.343316.

Pınar Çakır Hatır is an Associate Professor and Head of the Department of Biomedical Engineering at İstinye University, Istanbul, Turkey. She received her Bachelor of Science degree in Chemistry from Boğaziçi University in 2004, followed by a Master of Science in Chemistry from the same university in 2008. In 2012, she completed her doctoral studies in Biotechnology at Sorbonne Universities, University of Technology of Compiègne, in France, where she specialized in molecularly imprinted polymers and their innovative applications in nanomedicine. Her research interests lie at the intersection of nanomedicine, smart polymers, molecular recognition, and drug delivery systems, focusing on renewable resources for biomedical applications.

Alice Marinangeli is a PhD student in Biotechnology at University of Verona, and she is passionate about the development of sensors and their application in biomedical, industrial and environmental fields. Her expertise includes the synthesis and characterization of biomimetic polymers in a nanometric format by molecular imprinting technique. Alice is dedicated to use these polymers as synthetic receptor to design optical and electrochemical sensors.

Alessandra Maria Bossi has a MSc in Biochemistry (State University of Milano, Italy) and a PhD in Polymer Chemistry (Cranfield University, UK). AM Bossi founded and currently leads the Molecular Imprinting and Analytical Sciences Group at the Dept. of Biotechnology, University of Verona. Her research is dynamic and focuses on advancing the field of molecularly imprinted polymers (MIPs), where she has been pioneering innovations in both the synthesis and application of MIPs, including MIPs made starting from biological materials. AM Bossi's has received fundings by both public and private institutions, including the Italian Ministry of University and the European Union. She is regularly invited to international conferences and is author of more than 110 papers on peer review international journals and of 7 patents.

Gökhan Çaylı is a professor at Istanbul University-Cerrahpaşa, located in Istanbul, Türkiye. He obtained his Ph.D. from Boğaziçi University in 2008. His primary research focus is the synthesis of monomers and polymers derived from renewable resources as sustainable alternatives to petroleum-based materials. His expertise extends to photopolymerization, living polymerization techniques, polymer applications, and the study of interactions between nanoparticles and polymer structures.